https://doi.org/10.1016/j.jobe.2023.106961

Cross-infection risk assessment in dental clinic: numerical investigation of emitted droplets during different atomization procedures

Xiujie Li [a], Cheuk Ming Mak [a]*, Zhengtao Ai [b], Kuen Wai Ma [a], Hai Ming Wong [c]

a Department of Building Environment and Energy Engineering, The Hong Kong Polytechnic University, Hong Kong, China

b Department of Building Environment and Energy, College of Civil Engineering, Hunan University, Changsha, 410082, China

c Faculty of Dentistry, The University of Hong Kong, Hong Kong, China

*Corresponding author. Email address: cheuk-ming.mak@polyu.edu.hk

Abstract:

Cross-infection risk induced by the emitted droplets and bioaerosols during dental procedures has challenged service providers and patients alike. The present study aims to investigate the transmission mechanism of emitted droplets during the dental atomization procedures: vibration ultrasonic scaling (vUS) and rotation high-speed drilling (rHSD) and propose the risk assessment. Computational fluid dynamics (CFD) simulation was performed, and the experimentally recorded droplet velocity and diameter distribution during the atomization procedures were defined as initial boundary conditions. The droplet transmission in the dental clinic was analyzed from the final fate (deposition, suspension, and escape) and fallow time (FT) of emitted droplets. The results revealed that the diameter threshold for the droplet deposition and suspension was $60\ \mu m$, and the fraction of deposited droplets would be stable at 79.5% for rHSD and 85% for vUS. The primary contamination distance was generally within 0.28 m and 0.4 m from the treatment position for the atomization procedures of rHSD

and vUS, respectively. An increment of about 2% in the fraction of escaped droplets was noted when conducting the rHSD. The median of estimated FT for the atomization procedure of rHSD, 34 min, was longer than that of vUS, 30.6 min. In general, cross-infection risk during rHSD can be regarded as “higher” than vUS. The contribution of the present study can serve as guidance to decrease the cross-infection risk in dental clinics.

Keywords: Computational fluid dynamics (CFD); Dental atomization procedure; Droplet; Cross-infection risk; Dental clinic.

1. Introduction

Since the severe acute respiratory syndrome (SARS) epidemic swept the world in 2003, respiratory infectious disease outbreaks such as avian flu in 2005, swine influenza in 2009, and novel coronavirus disease 2019 (COVID-19) have emerged one after the other. The COVID-19 pandemic has substantially impacted economic development and the provision of medical services [1]. Based on the three documented transmission routes, including airborne transmission, droplet transmission, and direct contact [2], dental clinics have been widely treated as one of the most vulnerable healthcare organizations with a high cross-infection risk [3]. The spread of virus-laden droplets and bioaerosols generated during dental atomization procedures has attracted significant attention in recent months.

Although understanding of the severe acute respiratory syndrome coronavirus (SARS-CoV-2) has been deepened [4], there is still insufficient evidence to support policies to

reduce the possible infection risk in dental clinics [5]. Contrarily, the research field of dental aerobiology has been reported for over 50 years, and Micik first studied the relationship between dental professionals, patients, and aerosol particles [6]. Owing to the outbreak of COVID-19, plenty of experimental studies have been conducted to investigate droplet distribution through advanced equipment and methodologies. Li et al. [3, 7] employed the laser light scattering method to investigate the spatial-temporal distribution and airborne lifetime of the emitted droplets during ultrasonic scaling. Xing et al. [8] measured the bioaerosol concentration in the dental surgery room by the particle counter and found that the current mitigation measures were ineffective for high-momentum bioaerosols. Allison et al. [9] and Holliday et al. [10] investigated the contaminated region during dental procedures through the luminescent tracer and microbiological methods, respectively. Plog et al. [11] measured the diameter distribution and velocity of emitted droplets by the blacklight shadowgraph. However, considering the inherent limitations of point-based measurement by the particle counter and surface/plane recorded by the high-speed camera, the critical information about the airborne lifetime and the fraction of deposited and escaped droplets are inadequately reported. The aforementioned limitation of low spatial-temporal resolution studies poses a need to explore the detailed droplet transmission characteristics during different dental atomization procedures.

The fluid mixture in the oral cavity, including saliva, blood, and coolant water, would be rapidly atomized during dental procedures. However, the definition of dental atomization procedures still presents discrepancies among 72 countries [12], with

rotation high-speed drilling (rHSD) at 56% recognition and vibration ultrasonic scaling (vUS) at only 43%. Owing to the difference in atomization mechanisms, the initial diameter distribution and velocity of emitted droplets and bioaerosols would be inconsistent [13]. Several studies have been conducted to identify the diameter distribution of emitted droplets during different dental atomization procedures. For instance, Ou et al. [14] found that a bulk of the droplets were in the range of 12 - 200 μm during the atomization procedure of vUS. Similar droplet size distribution was also observed by Haffner et al. [15] using the optical flow tracking velocimetry method. Recently, Yuan et al. [13] experimentally compared the atomization mechanisms of the vUS and rHSD procedures and found a slight discrepancy in velocity but a significant difference in diameter distribution. The geometric mean diameter of emitted droplets during the atomization procedures of the vUS and rHSD was 42.5 μm and 25 μm, respectively. The smaller droplets and bioaerosols can be suspended in the air for much longer, increasing the mass fraction of inhalable particles and the probability of infection. Besides, different dental atomization procedures may lead to the ineffective performance of currently recommended mitigation measures. Li et al. [16] first proved the hypothesis about the moderate performance of the high-volume evacuation on high-velocity droplets and called for advancing targeted mitigation measures. Therefore, investigating the transmission mechanism of emitted droplets is of critical importance during different dental atomization procedures, which serves as the intrinsic basis for developing targerted mitigation measures. The quantitative infection risk between dental professionals and patients will help identify the risk level of dental atomization

procedures.

To quantitatively analyze the cross-infection risks in the dental clinic, the computational fluid dynamic (CFD) methods provide a convenient framework by investigating the droplet transmission and flow field characteristics [4, 17-19]. However, limited numerical studies have been conducted in the dental clinic owing to the model's complexity [20]. The oversimplifications, like the human microenvironment, droplet size distribution, and evaporation model, may lead to misunderstandings on droplet transmission and infection risk assessment [21-25]. For instance, Komperda et al. [21] investigated SARS-CoV-2 contamination in an open dental clinic, but they mainly focused on the effect of room ventilation without considering the human microenvironment. The thermal plume rising from the heated human body can directly impact the droplet dispersion around the human body [26], further affecting the cross-infection risk. Liu et al. [22] numerically studied the cross-infection risk in the dental environment by only considering the $1\ \mu m$ aerosol particles. Chen et al. [25] assessed the droplet dispersion in dental clinics without considering the evaporation effect. Since droplets in a wide-size distribution would be emitted during dental atomization procedures, some free-falling droplets gradually dehydrate, and the remaining non-volatile components form the droplet nuclei. Therefore, the aforementioned factors should be reasonably considered in future CFD studies.

Therefore, the present study aims to investigate the transmission mechanism of droplets emitted during the atomization procedures of the vUS and rHSD and propose a risk assessment. The droplet transmission in the dental clinic would be analyzed based on

the final fate (deposition, suspension, and escape) and fallow time (FT) of emitted droplets. The statistical data about the final fate of emitted droplets can help to identify the highly-contaminated region and the minimum required FT. The study can be regarded as necessary to help develop the targeted mitigation measures for different dental atomization procedures.

2. Model description

2.1 Computational geometry

The single dental surgery environment with dimensions of $x - y - z = 3.6\,m - 2.7\,m - 2.3\,m$ is numerically constructed, which is similar to the size of our previous experimental study [16]. The dental clinic is in the mixing ventilation, and the square supply and exhaust are located on both sides of the long axis of the ceiling. As shown in Fig. 1, a dental chair is located in the room center. The computational thermal manikin (CTM A) in red refers to the patient lying on the dental chair. The CTM B in blue represents the dental professional sitting next to the patient. The manikin models are obtained from a virtual manikin library [27]. The total surface area of CTM A and B is 1.74 m^2 and 1.68 m^2, respectively. The supply air temperature, ventilation rate, and relative humidity are maintained in line with our previous experimental study [16], which are the typical environmental conditions in dental clinics with air-conditioning systems. Two different dental atomization procedures, the vUS and rHSD, are separately conducted to investigate the spatial-temporal distribution and final fate of emitted droplets.

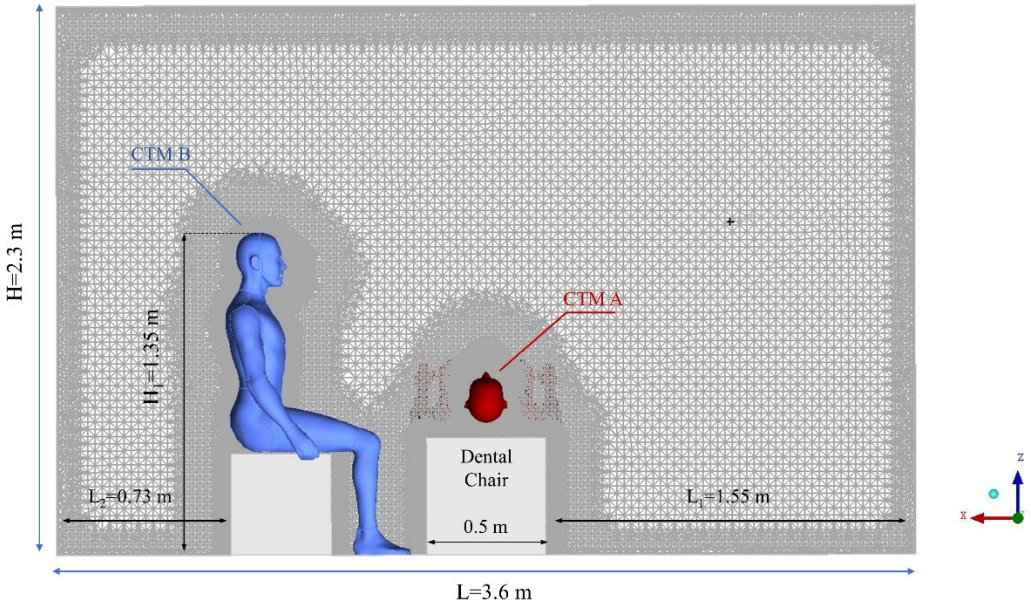

Fig. 1 Computational domain of the dental surgery environment: CTM A in red refers to the dental patient, and CTM B in blue represents the dental professional

3.2 Airflow phase model

CFD simulation in the present study is performed using the commercial software Ansys Fluent. The Realizable $k-\varepsilon$ turbulence model is adopted owing to its better performance in the velocity and contaminant prediction in the indoor environment [28]. The indoor air is modeled by the ideal-gas mixture of air and water vapor to reproduce the relative humidity in the dental surgery environment. The conservation equations of total mass, momentum, turbulent kinetic energy, turbulent dissipation rate, temperature, and species transport are discretized to obtain the steady-state solution of the initial flow field. Then the model would switch to a transient simulation. All the governing equations are discretized by the finite volume method. Pressure-implicit with the splitting of operators (PISO) algorithm is employed to couple the velocity and pressure field of the flow. The pressure equation is discretized using the "PRESTO" scheme, and

other equations are discretized using the second-order upwind scheme. The hybrid initialization by solving the $Laplace's$ equation is employed as the initial guess. The convergence is achieved by the residuals of continuity, momentum, turbulence, energy, and species below the order of 10^{-6}.

3.3 Discrete phase model

The Euler-Lagrange method is employed to track the trajectories and evaporation-induced size changes of the droplets in the dental surgery environment. The discrete phase model (DPM) and one-way coupling method are adopted to simulate droplet transmission in the air. The external forces acting on droplets should be equated with the inertia force (Newton's second law). The gravitation force, drag force, thermophoretic force, and Saffman's lift force are considered in the present study. The discrete random walk model is also employed to track the turbulent dispersion of droplets, allowing for the instantaneous fluctuating components on the droplet trajectories. Since the aforementioned models have been well-documented in the Fluent theory guide [29], plenty of research has been conducted using the method above [30-32]. The detailed equations are not presented. Once the mass of escaped droplets from ventilation and evaporated droplets reaches the constant, the DPM solution could be treated as converged.

The initial size distribution of the droplets generated during the atomization procedures of the vUS and rHSD on the central incisor has already been obtained from the laser light scattering method [13]. The diameter range of emitted droplets maintains in same from $5\,\mu m$ to $250\,\mu m$ for two the different atomization procedures, but the mean

diameter is quite different with the $42.5\ \mu m$ for the vUS and $24\ \mu m$ for the rHSD. In the DPM model, the Rosin-Rammler distribution is employed to fit the experimental size distribution of emitted droplets, following the equation: $Y_D = e^{-(D/\overline{D})^n}$, where the Y_D is the mass fraction of droplets of diameter larger than D; $\overline{D}$ is the mean diameter, and n is the spread parameter. Fig. 2 shows the experimental size distribution of droplets during dental atomization procedures compared to the Rosin-Rammler distribution in the DPM model. The velocity of emitted droplets during the vUS and rHSD is maintained at $2.63\ m/s$ and $2.22\ m/s$, respectively. The aforementioned velocity and diameter distrbution characteritics of emitted droplets were measured, when the coolant water flow rate were kept at $60\ ml/min$ [13].

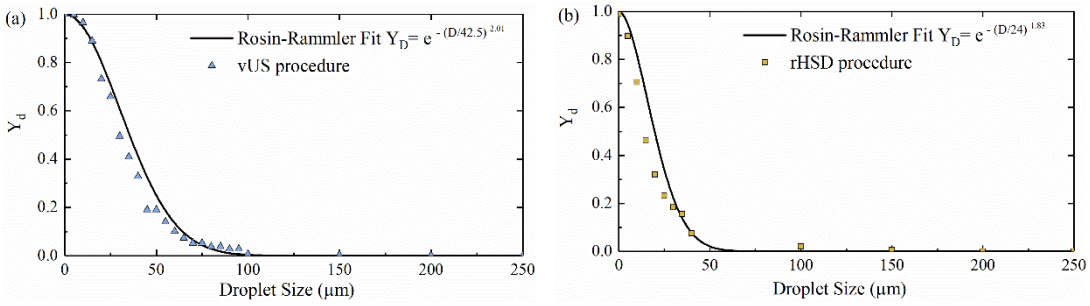

Fig. 2 Experimental size distribution of droplets during dental atomization procedures compared to the Rosin-Rammler distribution in the DPM model: a) Atomization procedure of vUS; b) Atomization procedure of rHSD

During dental atomization procedures, volatile and non-volatile components are present in the emitted droplets. The droplets' diameter gradually decreases when the droplet temperature is higher than the vaporization temperature. Several experimental studies have investigated the evaporation rate and final diameter of human respiratory droplets [33-37]. For the present study, the size of the evaporated droplet nuclei provided by

191 Basu et al. [37] is around 26% of the initial droplet diameter for the studied relative
192 humidity range. Therefore, the droplets are modeled to be composed of 98.2% water
193 ($\rho = 998\ kg/m^3$) and 1.8% salt ($\rho = 2170\ kg/m^3$). To the best of our knowledge,
194 more accurate estimates about the size of the evaporated droplet nuclei in dental clinics
195 are still unknown. The evaporation characteristics of coughing-generated droplets have
196 been systematically investigated [36, 38]. Under the assumption that coolant water does
197 not dilute the saliva [21], the evaporation properties of dental-emitted droplets can be
198 treated in line with those of coughing generated.

199 **3.4 Boundary conditions**

200 The setting of human breathing flow and thermal plume should be accurately defined
201 to reproduce the human micro-environment. Even in the same environmental
202 temperature, the surface temperature of different human body segments also presents a
203 difference (larger than 3℃) [39]. In addition, the division of CTM's body segments
204 can help to identify the contamination region when droplets are deposited on the human
205 body. Therefore, the CTMs are divided into four segments (shown in Fig. 3a): head,
206 arm, torso, and leg, where the CTM's head and arm are exposed to the ambient
207 environment. Based on the results of the previous experimental study [40], the heat
208 power of each CTM is defined as 80 W. The convective and radiation heat load ratio is
209 3:7 [41]. Thus, a convective heat load of 24 W is employed in the present study without
210 considering the radiation effect. A summary of boundary conditions is presented in
211 Table 1.

212

213 Table 1 Summary of boundary conditions

Airflow phase	Air supply	Velocity inlet, Temperature=27 ℃, RH= 50%, ACH=6 h^{-1}
	Air exhaust	Outflow
	Human body	Total heat power of 80 W
	Room wall	Adiabatic
Discrete phase	Patient's mouth	$V_{vUS} = 2.63\ m/s, V_{rHSD} = 2.22\ m/s$, Injection type: cone; Injection angle =30°; Mass flow rate=0.001 kg/s
	Droplet sizes	Range: $5 - 250\ \mu m$, $D_{mean-vUS} = 42.5\ \mu m$, $D_{mean-rHSD} = 24\ \mu m$
	Composition & density	98.2% water ($\rho = 998\ kg/m^3$) and 1.8% salt ($\rho = 2170\ kg/m^3$), Density=1000 kg/m^3
	Temperature	Temperature=37 ℃
	Inlet	Escape
	Outlet	Escape

214 The definition of CTM breathing conditions can directly impact the cross-infection risk
215 assessment between dental professionals and patients. In addition, the nasal breathing
216 flow of the dental patient would directly act on the droplet ejection from the treatment
217 region. Therefore, the dental patient is set as the nose inhalation/exhalation during the
218 dental atomization procedures, while the dental professional is set as mouth
219 inhalation/exhalation. Since the present study only focuses on the worst condition,

susceptible subjects (dental professionals) breathing through the mouth can induce high cross-infection risks [42, 43]. The respiratory rate of nasal breathing flow is set as 6 L/min, and the two jets are inclined 45° downwards from the vertical plane and 30° from each other [44]. The cross-sectional area of each nostril is $38.5\,mm^2$ [40]. As shown in Fig. 3b, each breathing cycle is composed of inhalation (2.5 s), exhalation (2.5 s), and break (1.0 s) [45, 46]. The User-defined function is employed to set the nasal breathing conditions, and the breathing flow against time is a sinusoidal curve: $V = 0.1884\sin(1.256t)$, where V refers to the flow rate, L/s; t is the time, s. Non-slip wall with enhanced wall treatment is applied for all wall surfaces. When droplets encounter a surface, two distinctive fates are presented: trap and escape. All building wall, floor, dental chair and human segments are assigned with the "trap" condition. Once the droplets are deposited on the aforementioned surfaces, they would not re-suspend in the air. "Escape" condition is used for the ventilation inlet, outlet, dental patient's noses and dental professional's mouth.

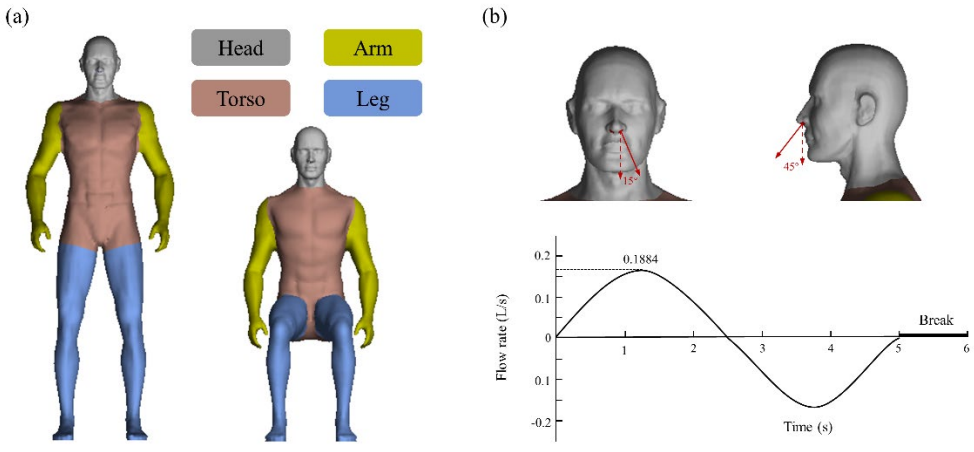

Fig. 3 a) Division of CTM body segments; b) Nasal breathing settings of the dental patient

3. CFD simulation

3.1 Grid independence test

A grid independence test is then conducted by the three polyhedron-based grids, namely fine: 14.2 million, medium: 8.8 million, and coarse: 4.6 million. The comparison of dimensionless velocity profiles along the measurement line E-F is presented in Fig. 4 based on the three sets of grids. A similar variation in velocity with distance is found for the three grids. The average relative deviation of the velocity magnitudes between the medium and coarse grids is 22.5%, and the relative deviation between the fine and medium grids is only 1.2%. Since the difference between the fine and medium grids is tiny, the medium grid of 8.8 million is employed in the study to balance the computational cost and accuracy of the results.

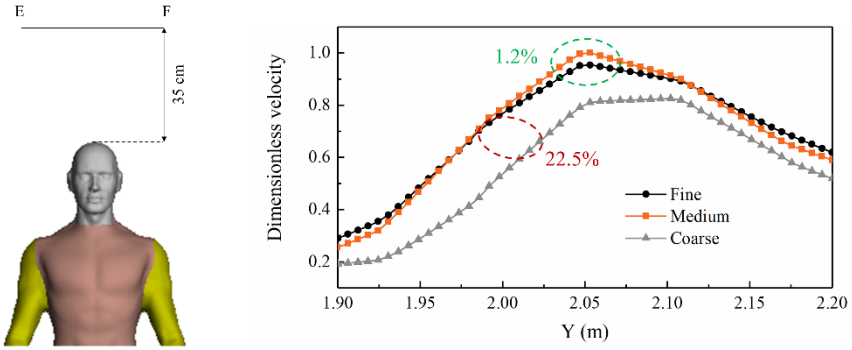

Fig. 4 Grid independence test by comparing the dimensionless velocity magnitude along the measurement line E-F

3.2 Model validation

Cross-infection risk between dental professionals and patients is significantly impacted by the evaporation process of droplets, which is driven by the difference between the equilibrium vapor pressure of the droplet surface and the partial pressure of the water

vapor in ambient air. The results are compared with the studies of Li et al. [35] and Redrow et al. [36] to validate the evaporation model. The experimental chamber maintained a fixed temperature of 25 ℃. Droplets with two different initial diameters of $10\,\mu m$ and $100\,\mu m$ descend in the quiescent air and dry condition. Single droplets of the temperature of 37 ℃ were sequentially released with a time resolution of 0.01s. Droplets were defined with a density of 1000 kg/m^3, containing 98.2 % water and 1.8 % non-volatile materials. As shown in Fig. 5, a satisfactory agreement can be noticed between the predicted time-dependent droplet diameter (solid line) and data reported in the literature. The normalized mean square error (NMSE) and fraction bias (FB) are employed as evaluation metrics to quantify the reliability of the model validation.

$$NMSE = \frac{\overline{(M_i - C_i)^2}}{\bar{M}\,\bar{C}} \tag{1}$$

$$FB = \frac{\bar{M} - \bar{C}}{0.5(\bar{M} + \bar{C})} \tag{2}$$

where M_i and C_i refer to the measured and computed values for the sample i. The maximum calculated values of the NMSE and $|FB|$ are respectively 0.022 and 0.13, which satisfies the recommended criteria ($NMSE \leq 4$ and $|FB| \leq 0.3$) in Li et al. [47]. The evaporation rate is significantly affected by the initial droplet diameter. The required time for $10\,\mu m$ droplets is less than 0.1 s to dehydrate as droplet nuclei, while about 4 min is needed for the $100\,\mu m$ droplets. The results indicate that the present CFD simulation can reasonably predict the evaporation process of droplets. In the dental surgery environment, the diameter distribution of emitted droplets during different atomization procedures is quite discrepant, further impacting their

277 corresponding transmission patterns. The results of the present study would advance
278 knowledge about dental atomization procedures and promote the development of
279 targeted mitigation measures.

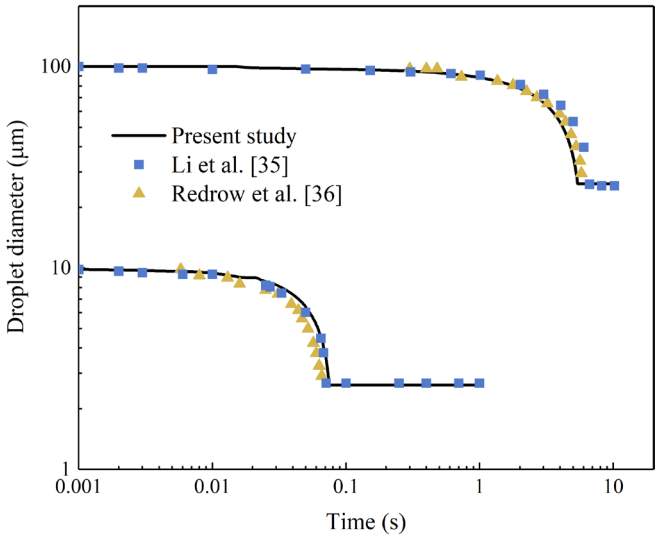

280

281 Fig. 5 Model validation of droplet evaporation compared with the studies of Li et al.
282 [35] and Redrow et al. [36]

283 **4. Results**

284 **4.1 Flow field analysis**

285 The analysis of the flow field serves as the foundation for the subsequent research on
286 the transmission of emitted droplets. Fig. 6a shows the velocity vector and velocity
287 streamlines on the plane ($y = 2.035\ m$), crossing the dental professional's mouth and
288 dental treatment region. Fresh air enters the dental environment through the ceiling inlet,
289 along with the interaction with the human thermal plume. An apparent velocity
290 fluctuation is presented near the human body owing to the temperature difference.
291 Finally, the mixed air is expelled through the ceiling outlet. The distribution of turbulent
292 kinetic energy (TKE) in the dental clinic is presented in Fig. 6b. Generally, a high TKE
293 region refers to considerable fluctuations in root mean square velocity [21]. The higher

magnitude TKE is presented on the left side of the dental surgery environment and around the dental professional. The difference in TKE between the left and right sides of the room could cause an imbalance in the flow characteristics in the dental clinic, further significantly impacting the distribution of generated droplets and aerosol particles (detailed analysis in Section 4.2).

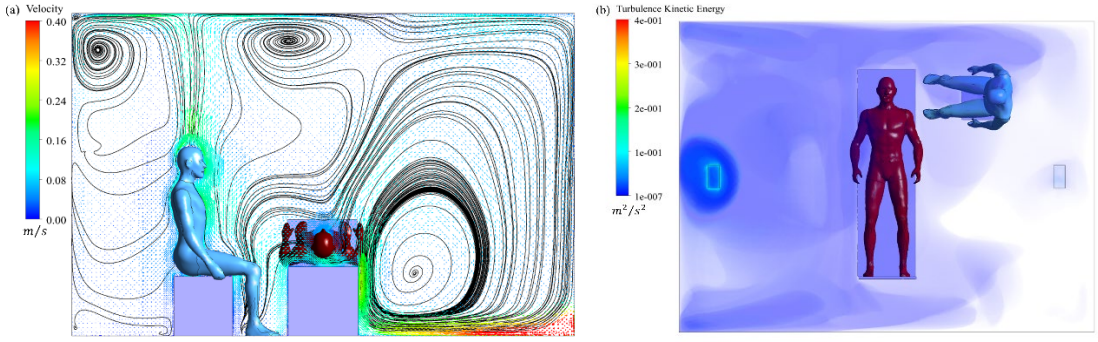

Fig. 6 a) Velocity vector and velocity streamlines on the plane ($y = 2.035\ m$); b) Non-uniform distribution of turbulent kinetic energy in the dental surgery environment

4.2 Droplet characteristics

4.2.1 Spatial-temporal distribution of emitted droplets

Airborne transmission of respiratory diseases causes significant concern about the residence time, final fate, and proportion of emitted droplets in dental surgery environments. Fig. 7 compares the spatial-temporal distribution of generated droplets during the dental atomization procedures of vUS and rHSD. Since the diameter range of emitted droplets ($5 - 250\ \mu m$), ambient relative humidity (50%), and temperature (27℃) are maintained in the same, the diameter threshold for the droplet deposition and suspension is identified as $60\ \mu m$. It is calculated based on the maximum diameter of remaining non-volatile components ($15.6\ \mu m$ after 10 min) and the volatile mass

fraction. Some of those smaller droplets, with an initial diameter $< 60\ \mu m$, gradually dehydrate and move with the flow. Smaller droplets almost saturate the entire dental environment after the cessation of atomization procedures (2 min). As illustrated, the smaller droplets first move along the ejection path, then rise following the thermal plume near the dental patient, and spread with the ambient ventilation flow. By contrast, different transmission behavior is noted for the larger droplets $> 60\ \mu m$. Owing to their large initial momentum, the larger droplets would travel a longer distance even when subjected to the drag force induced by the air. After losing their initial momentum, gravity acting as the dominant force on droplets would lead to deposition near the dental treatment region. For example, a majority of larger droplets over $60\ \mu m$ would be deposited on the patient's chest (0.634 s on average) and dental chair (5.19 s on average) during the atomization procedure of the vUS. After about 30 min, the mass of evaporated and escaped droplets maintains nearly constant with the converged DPM solution.

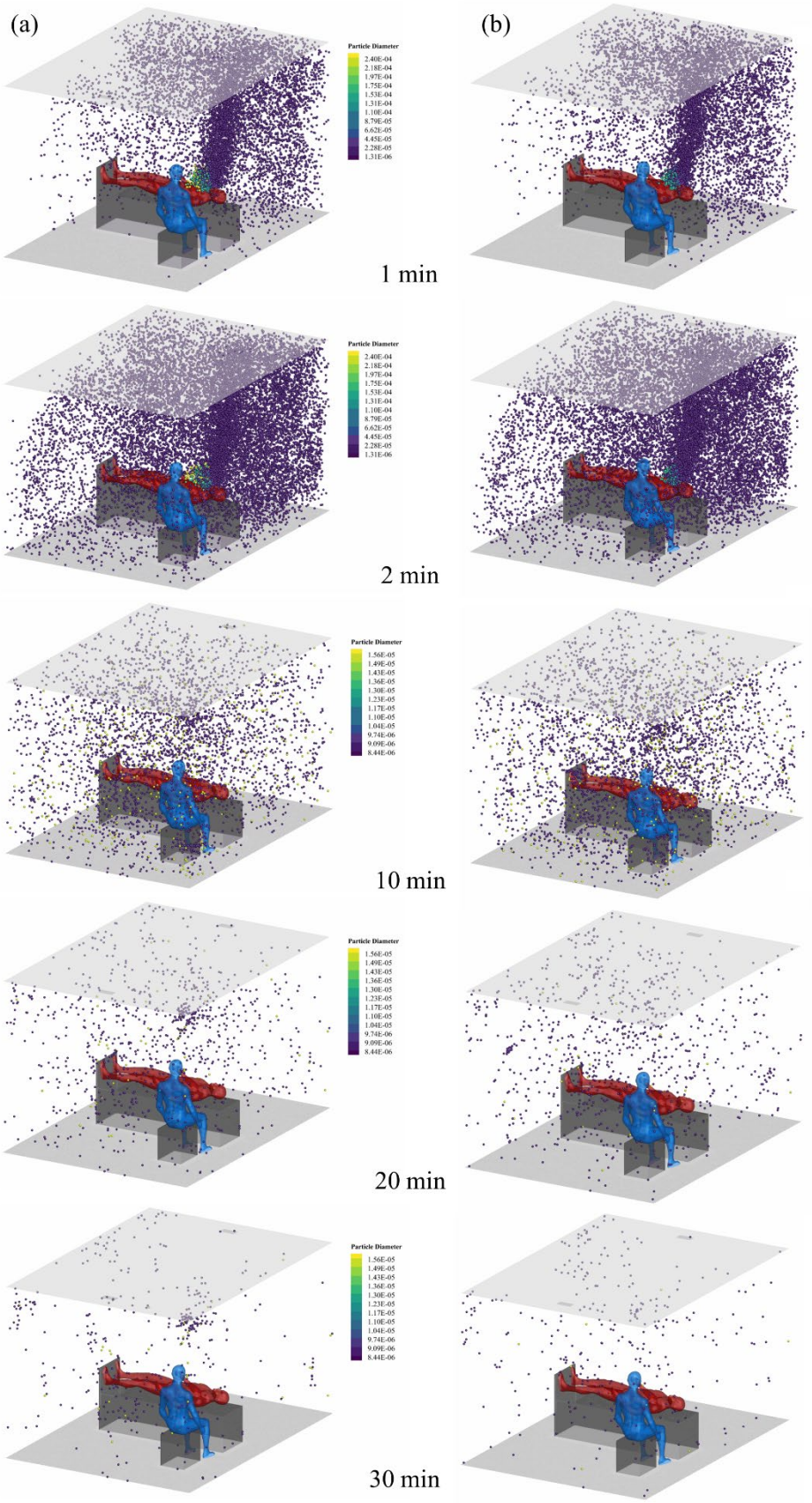

Fig. 7 Comparison of the spatial-temporal distribution of emitted droplets under the

dental atomization procedures: a) vUS and b) rHSD

The flow field characteristics can directly impact the spatial-temporal distribution of generated small droplets. Higher droplet concentration resides on the left side of the dental environment with the increased TKE (shown in Fig. 7). The observation of the particle behavior is in line with prior studies [21, 48, 49], indicating that the emitted inertial particles would concentrate in high-strain regions. Our previous experimental study also observed a spatial region with high droplet mass concentration [16]. Avoiding direct exposure to dental professionals should be highly noticed. In addition, the decontamination and disinfection inside the dental surgery environment should be extended to cover all possible surfaces. The cooperation of dental suction equipment has been confirmed to help remove the high-strain region [16], further reducing the number of emitted droplets and areas of the contaminated region.

4.2.2 Final fate and proportion of emitted droplets

Generally, three distinct fates are considered for the emitted droplets during the dental atomization procedures. Some droplets are deposited on surfaces, some escape the computational domain, and the rest become suspended in the dental surgery environment. Fig. 8 presents the fraction of escaped and deposited droplets after the dental atomization procedures of vUS and rHSD. As illustrated, different dental atomization procedures significantly affect the final fate and proportion of emitted droplets. The rHSD, with a higher fraction of escaped droplets, indicates fewer droplets left inside the dental environment. After 30 min, the fraction of escaped droplets is stabilized at 4.2% for vUS and 6.1% for rHSD. An increment of about 2% in the fraction

of escaped droplets is noticed when conducting the rHSD. The result about the fraction of escaped droplets is generally in line with a prior study conducting the atomization procedure of vUS in a large dental clinic, with an escape rate of 3.953% [21]. Smaller droplets generated during the dental atomization procedures would follow the flow streamlines created towards the ventilation exhaust. The virus-laden droplets entering the air-conditioning system may lead to possible transmission in dental clinics, and the disinfection of the air-conditioning system should be conducted. In Fig. 8b, the fraction of deposited droplets increases progressively with time and remains constant for around 30 min. That would be stable at about 79.5% for rHSD and 85% for vUS.

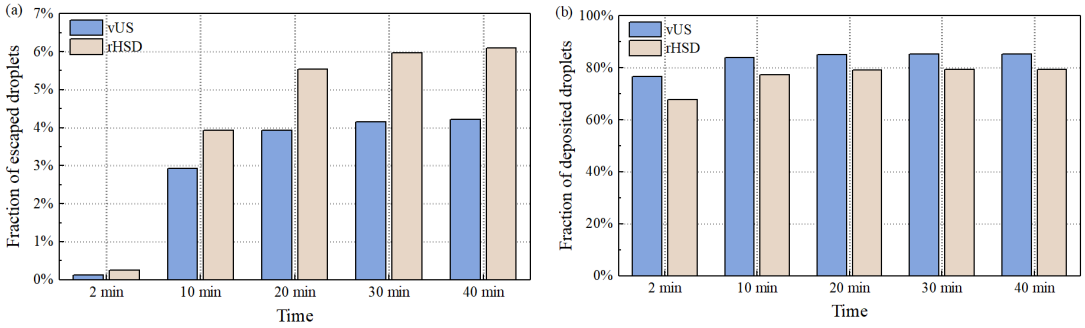

Fig. 8 Fraction of escaped and deposited droplets after the different dental atomization procedures: a) the vUS and b) the rHSD

Fig. 9 shows the detailed deposition location of the emitted droplets during the dental atomization procedures of rHSD and vUS at 40 min. As illustrated, a vast majority of droplets would deposit on the patient's torso, accounting for about 44.3% during the rHSD and 62.5% during the vUS. The following deposition regions are the floor and the patient's head. For example, for the atomization procedure of rHSD, approximately 19.4 % and 10.7% of emitted droplets would be deposited on the floor and the patient's head. The primary contamination distance for larger droplets (> 60 μm) during the

atomization procedures of rHSD and vUS is generally within 0.28 m and 0.4 m from the treatment position, respectively. The initial momentum of emitted droplets could account for the difference in the area of the contaminant region during different dental procedures. The results about the contaminant regions are in line with previous experimental studies using the luminescent tracer and microbiological methods [10, 50]. As for smaller droplets (< 60 μm), some would be concentrated in high-strain regions (shown in Fig. 6b). With time development, they would gradually deposit in the dental floor and escape from the ventilation exhaust. A higher density of droplet deposition resides on the left side of the dental environment due to the increased TKE (shown in Fig. 7). It highlights that the decontamination and disinfection inside the dental surgery environment should be extended to cover all possible surfaces.

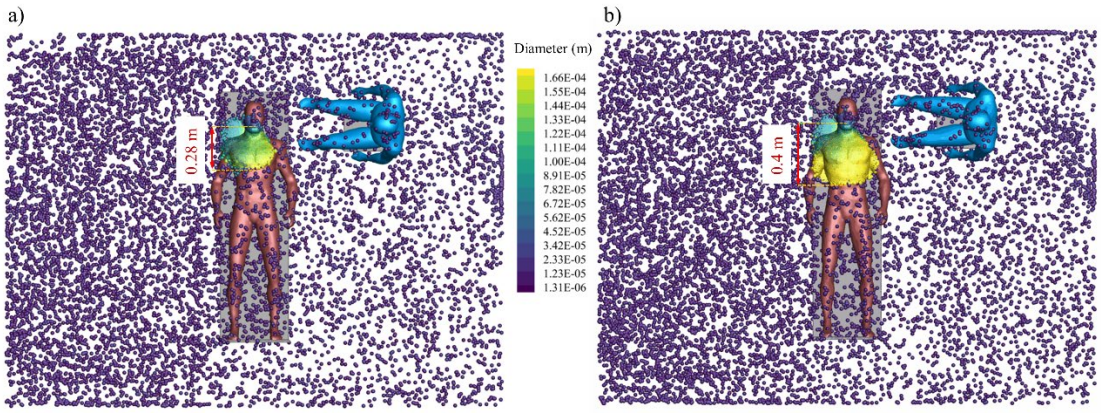

Fig. 9 Deposition location of the emitted droplets at 40 min after the different dental atomization procedures: a) the rHSD and b) the vUS

4.3 Fallow time (FT) determination and infection risk

In the dental surgery environment, FT is defined as the time taken for the number of suspended droplets to drop to a defined safe level after dental atomization procedures are completed for dental patients. One challenge in the dental surgery environment is

balancing the minimum required FT and the number of daily appointments, thereby removing the fear and uncertainty associated with the possible airborne transmission of diseases. Fig. 10 presents the decay curve of droplet count on the central room plane ($x = 1.8\ m$) and the estimated FT under different atomization procedures of vUS and rHSD. The blue shadow zone is the measured FT in our previous experimental study using the laser light scattering method on the central room plane [7], with a median FT of 30.6 min (range 27–35 min). The FT result for the vUS procedure is in line with many previous studies using the point-based measurement of the particle counter [9, 51, 52]. Based on the baseline level defined by the vUS procedure in the same dental environment, the median FT for the rHSD can be predicted for appropriately 34 min. The results are consistent with a previous study that indicated that a more extended FT was required for the atomization procedure of rHSD to reduce the aerosol concentration level [53]. Therefore, the FT determination in dental clinics should consider the different dental treatment plans and atomization mechanisms.

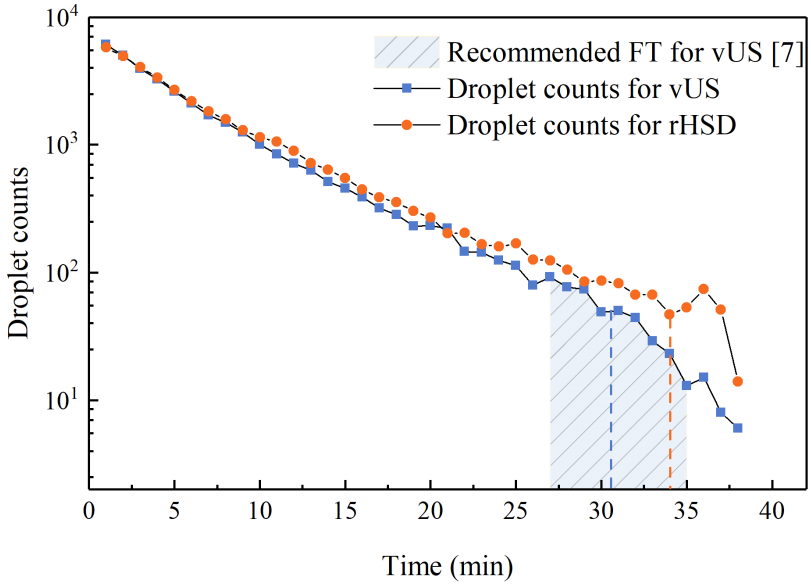

Fig. 10 Decay curves of droplet count and the estimate FT under different dental

atomization procedures of vUS and rHSD

Cross-infection risk for dental atomization procedures is estimated by calculating the viral load of droplets in the dental professional's breathing zone. The breathing zone proposed under transient breathing conditions is employed in the present study [47, 54]. Droplets emitted during the rHSD take more time to the dental professional's breathing zone than those generated during the vUS. For example, the average time for droplets presented in the dental professional's breathing zone is 6.03 min and 7.34 min for the atomization procedures of vUS and rHSD, respectively. As for the cross-infection risk, the viral load of SARS-CoV-2 in droplets is assumed to be proportional to the initial size of the droplet and is unaffected by droplet dehydration. Owing to the lack of studies on the viral load in the emitted droplets during dental procedures, the median SARS-CoV-2 viral load ($3.3 \times 10^6\ copies/ml$) proposed by To et al. [55] in saliva specimens are employed. The breathing zone of the dental professional could contain upwards of $0.017\ \mu l$ saliva and $0.0216\ \mu l$ saliva for the atomization procedures of vUS and rHSD, respectively. Upwards of $4.3 \times 10^5\ copies/m^3$ of the virus are contained in the dental professional's breathing zone for the rHSD. The results are generally in line with previous microbiological risk assessments of $0.014\ \mu l$ of aerosolized saliva [56]. Overall, based on the final fate of emitted droplets and minimum required FT, cross-infection risk during the atomization procedure of rHSD can be regarded as "higher" than that of vUS. Notably, the current estimation is based on the worst-case scenarios without the cooperation of precautionary measures like personal protective equipment, high-volume evacuation, and air purifiers.

5. Discussion

Droplets and bioaerosols emitted during dental atomization procedures may promote the cross-infection of diseases among dental professionals and patients. However, to the best of our knowledge, there are at least three primary questions with no clear quantitative answers. Question 1: What is the limit aerosol concentration that could be considered a safe operation room? In other words, the minimum required FT between two appointments should be established when finishing the dental atomization procedures in the confined surgery room. Clearly, this would be determined by plenty of parameters like ventilation rates, droplet emission characteristics induced from the procedure types, duration time, and treatment region. Especially concerning the droplet emission characteristics during different dental atomization procedures, the information available in the scientific literature is relatively scarce [57]. Question 2: how about the actual performance of the recommended mitigation measures on the droplets emitted during different dental atomization procedures? In the case of insufficient ventilation, the moderate effect of high-volume evacuation on the large and high-velocity droplets has been proven [16], and they called for the advancement in developing targeted mitigation measures. Question 3: Which dental atomization procedures would induce the “higher” cross-infection risk in the dental surgery environment? Owing to the difference in atomization mechanisms, the initial diameter distribution and velocity of emitted droplets would be inconsistent [13]. Besides, the definition of dental atomization procedures still presents discrepancies among countries [12], with the recognition of rHSD at 56% and vUS at only 43%. Therefore, the present study aims to

449 answer the first and third questions. From the decay curves of droplet count (Fig. 10)
450 in the same ambient environmental conditions, the estimated FT for the rHSD
451 procedure is 4 min longer than that for the vUS procedure. The results are consistent
452 with a previous study that required a more extended FT for the rHSD procedure to
453 reduce the aerosol concentration level [53]. Based on comparing the final fate of
454 emitted droplets and cross-infection risk assessment, cross-infection risk during the
455 atomization procedures of the rHSD can be regarded as “higher” than that of the vUS.
456 The aforementioned quantitative assessment can serve as guidance to decrease the
457 cross-infection risk in dental clinics and develop targeted mitigation measures for
458 different dental atomization procedures.
459 Plenty of mitigation measures have been proposed to reduce the cross-infection risk
460 between dental professionals and patients, shown in the literature with better
461 performance in limiting disease transmission. Those include the negative pressure room,
462 personal ventilation, the dental dam, high-volume evacuation, enhanced filtration,
463 protective chamber, and air purifiers [58-60]. The high-volume evacuation was
464 recommended at the beginning of the pandemic. It is a suction device that draws a large
465 volume of air along with droplets and aerosol particles. Recently, Li et al. [16] used the
466 laser light scattering method and found its moderate effect on large, high-velocity
467 droplets. Notably, these high-momentum particles are a significant source of prolonged
468 suspended particulate matter in the dental surgery environment, increasing the mass
469 fraction of inhalable particles and the probability of infection. Air purifiers equipped
470 with high-efficiency particulate air filters have been suggested as the supplemental

mitigation measure to reduce the cross-infection risk during the current severe COVID-19 pandemic [61]. Rodríguez et al. [62] employed the real-time RT-PCR method to investigate the virus concentration in households and found that the air purifiers can effectively decrease the viral RNA from room air, thus further reducing the risk of airborne transmission. However, the application of air purifiers in the dental clinics of Hong Kong is relatively rare, even though the COVID-19 pandemic is already more than two-year. Besides, the effect of these combined strategies, like high-volume evacuation, air purifiers, and ventilation, is not well-explored in dental clinics. Investigating the aforementioned combined strategies is necessary to further reduce the potential infection risk.

Further reducing the emitted droplets is critical to quickly restore the global healthcare system, especially for routine medical and dental procedures. Recently, Hong Kong Dental Association pointed out that dental professionals and assistants with appropriate personal protective equipment when performing dental atomization procedures would not be classified as having close contact with confirmed patients [63]. Although personal protective equipment performs better in shielding dental professionals, the long airborne lifetime of suspended droplets still calls for the need to institute the FT between appointments. Establishing FT in dental clinics can protect dental patients' health and well-being. Besides, due to the absence of negative-pressure rooms, many dental clinics, especially those in old commercial buildings, rely only on the heating, ventilation, and air-conditioning system alone [64]. From the results of the present study, the fraction of escaped droplets from the ventilation system can reach 6.1% for the

493 atomization procedure of rHSD. The air-conditioning system in dental clinics should
494 be decontaminated to avoid possible transmission. Besides, a vast majority of droplets
495 become deposited, with 79.5% for the rHSD and 85% for the vUS. Disinfection should
496 be extended to cover all possible surfaces in the dental surgery environment.
497 Saliva is rheologically complicated and varies from person to person [65]. In the present
498 study, coolant water during dental atomization procedures is assumed to not dilute the
499 saliva, owing to the limited investigation on the evaporation characteristics of dental-
500 emitted droplets. Future research is warranted to verify the assumption. As for the viral
501 load in the emitted droplets in the dental surgery environment, the median SARS-CoV-
502 2 viral load ($3.3 \times 10^6\ copies/ml$) in saliva specimens are employed [55]. The size
503 distribution and velocity of the emitted droplets are obtained from the experiments
504 carried out on the central incisor, where the vast majority of droplets would be emitted
505 from the patient's oral cavity. Different treatment regions would directly impact the
506 characteristics of emitted droplets, but the present study can be regarded as the worst-
507 case scenario. The results of the present study could serve as guidance to advance our
508 understanding of disease transmission in dental clinics and further help develop the
509 target mitigation measures.

510 **6. Conclusion**

511 The present study investigates the transmission mechanism of droplets emitted during
512 the atomization procedures of the rHSD and vUS, with a particular focus on the final
513 fate and FT of the emitted droplets. Cross-infection risk assessment in the dental clinic
514 has also been proposed. The results can help protect dental professionals' and patients'

health and well-being.

Some meaningful conclusions can be stated:

1) Diameter threshold for the droplet deposition and suspension can be identified as 60 μm, and the fraction of deposited droplets would be stable at 79.5% for rHSD and 85% for vUS. The primary contamination distance was generally within 0.28 m and 0.4 m from the treatment position for the atomization procedures of rHSD and vUS, respectively.
2) Owing to the discrepancy in droplets' velocity and diameter distribution during different atomization procedures, the fraction of escaped droplets for the rHSD (6.1%) was higher than that for the vUS (4.2%). The air-conditioning system in dental clinics should be decontaminated to avoid possible transmission.
3) Without cooperating mitigation measures, the median of estimated FT for the atomization procedure of rHSD, 34 min, was longer than that of vUS, 30.6 min. Cross-infection risk during rHSD can be regarded as “higher” than vUS.

Declaration of competing interest

The authors declare that they have no known competing financial interests or personal relationships that could have appeared to influence the work reported in this paper.

Acknowledgments

This study was supported by the National Natural Science Foundation of China (No. 51908203) and the Fundamental Research Funds for the Central Universities (No. 531118010378).

Reference

1. Akbari, P., et al., *Housing and mental health during outbreak of COVID-19.* Journal of Building Engineering, 2021. **43**: p. 102919.
2. Wang, C.C., et al., *Airborne transmission of respiratory viruses.* Science, 2021. **373**(6558): p. eabd9149.
3. Li, X., et al., *Evaluating flow-field and expelled droplets in the mockup dental clinic during the COVID-19 pandemic.* Physics of Fluids, 2021. **33**(4): p. 047111.
4. Tsang, T.-W., K.-W. Mui, and L.-T. Wong, *Computational Fluid Dynamics (CFD) studies on airborne transmission in hospitals: A review on the research approaches and the challenges.* Journal of Building Engineering, 2022: p. 105533.
5. Sergis, A., et al., *Mechanisms of atomization from rotary dental instruments and its mitigation.* Journal of dental research, 2021. **100**(3): p. 261-267.
6. Micik, R.E., et al., *Studies on dental aerobiology: I. Bacterial aerosols generated during dental procedures.* Journal of dental research, 1969. **48**(1): p. 49-56.
7. Li, X., et al., *Restoration of dental services after COVID-19: The fallow time determination with laser light scattering.* Sustainable Cities and Society, 2021. **74**: p. 103134.
8. Xing, C., et al., *Spatiotemporal distribution of aerosols generated by using powder jet handpieces in periodontal department.* Sustainable Cities and Society, 2021. **75**: p. 103353.
9. Allison, J.R., et al., *Evaluating aerosol and splatter following dental procedures: Addressing new challenges for oral health care and rehabilitation.* Journal of oral rehabilitation, 2021. **48**(1): p. 61-72.
10. Holliday, R., et al., *Evaluating contaminated dental aerosol and splatter in an open plan clinic environment: Implications for the COVID-19 pandemic.* Journal of dentistry, 2021. **105**: p. 103565.
11. Plog, J., et al., *Reopening dentistry after COVID-19: Complete suppression of aerosolization in dental procedures by viscoelastic Medusa Gorgo.* Physics of Fluids, 2020. **32**(8): p. 083111.
12. Clarkson, J., et al., *Aerosol generating procedures and their mitigation in international dental guidance documents-a rapid review.* Cochrane Oral Health, 2020: p. 1-69.
13. Yuan, C., et al., *Spatiotemporal distribution and control measure evaluation of droplets and aerosol clouds in dental procedures.* Infection Control & Hospital Epidemiology, 2022: p. 1-3.
14. Ou, Q., et al., *Characterization and mitigation of aerosols and spatters from ultrasonic scalers.* The Journal of the American Dental Association, 2021. **152**(12): p. 981-990.
15. Haffner, E., et al., *An experimental approach to analyze aerosol and splatter formations due to a dental procedure.* Experiments in Fluids, 2021. **62**(10): p. 1-17.
16. Li, X., et al., *How the high-volume evacuation alters the flow-field and particle removal characteristics in the mock-up dental clinic.* Building and Environment, 2021. **205**: p. 108225.
17. Dai, Y., F. Zhang, and H. Wang, *Identification of source location in a single-sided building with natural ventilation: Case of interunit pollutant dispersion.* Journal of Building Engineering, 2023: p. 106049.
18. Ye, J., Z. Ai, and C. Zhang, *A new possible route of airborne transmission caused by the use of a physical partition.* Journal of Building Engineering, 2021. **44**: p. 103420.

19. Wu, J., et al., *Numerical study of transient indoor airflow and virus-laden droplet dispersion: Impact of interactive human movement.* Science of The Total Environment, 2023: p. 161750.
20. Li, X., et al., *Numerical investigation of the impacts of environmental conditions and breathing rate on droplet transmission during dental service.* Physics of Fluids, 2023. **35**(4): p. 043332.
21. Komperda, J., et al., *Computer simulation of the SARS-CoV-2 contamination risk in a large dental clinic.* Physics of Fluids, 2021. **33**(3): p. 033328.
22. Liu, Z., et al., *Bioaerosol distribution characteristics and potential SARS-CoV-2 infection risk in a multi-compartment dental clinic.* Building and Environment, 2022. **225**: p. 109624.
23. Nambu, E., et al., *Numerical simulation of air age in dental offices.* Scientific Reports, 2022. **12**(1): p. 1-7.
24. Zhang, W., C.M. Mak, and H. Wong, *Pollutant dispersion in a natural ventilated dental clinic.* Building Services Engineering Research and Technology, 2013. **34**(3): p. 245-258.
25. Chen, C., et al., *The effectiveness of an air cleaner in controlling droplet/aerosol particle dispersion emitted from a patient's mouth in the indoor environment of dental clinics.* Journal of the Royal Society Interface, 2010. **7**(48): p. 1105-1118.
26. Zong, J., et al., *A review of human thermal plume and its influence on the inhalation exposure to particulate matter.* Indoor and Built Environment, 2022: p. 1420326X221080358.
27. Yoo, S.J. and K. Ito, *Validation, verification, and quality control of computational fluid dynamics analysis for indoor environments using a computer-simulated person with respiratory tract.* Japan Architectural Review, 2022. **5**(4): p. 714-727.
28. ANSYS, I., *ANSYS Fluent Theory Guide*. Realizable k-epsilon model. 2020: ANSYS, Inc., Canonsburg, PA.
29. ANSYS, I., *ANSYS Fluent Theory Guide*. Turbulent Dispersion of Particles. 2020: ANSYS, Inc., Canonsburg, PA.
30. Ji, Y., et al., *The impact of ambient humidity on the evaporation and dispersion of exhaled breathing droplets: A numerical investigation.* Journal of aerosol science, 2018. **115**: p. 164-172.
31. Chen, C. and B. Zhao, *Some questions on dispersion of human exhaled droplets in ventilation room: answers from numerical investigation.* Indoor Air, 2010. **20**(2): p. 95-111.
32. Blocken, B., et al., *Towards aerodynamically equivalent COVID19 1.5 m social distancing for walking and running.* preprint, 2020.
33. Lieber, C., et al., *Insights into the evaporation characteristics of saliva droplets and aerosols: levitation experiments and numerical modeling.* Journal of Aerosol Science, 2021. **154**: p. 105760.
34. Chaudhuri, S., et al., *Modeling the role of respiratory droplets in Covid-19 type pandemics.* Physics of Fluids, 2020. **32**(6): p. 063309.
35. Li, X., et al., *Modelling of evaporation of cough droplets in inhomogeneous humidity fields using the multi-component Eulerian-Lagrangian approach.* Building and Environment, 2018. **128**: p. 68-76.
36. Redrow, J., et al., *Modeling the evaporation and dispersion of airborne sputum droplets expelled from a human cough.* Building and Environment, 2011. **46**(10): p. 2042-2051.
37. Basu, S., et al., *Insights on drying and precipitation dynamics of respiratory droplets from the perspective of COVID-19.* Physics of Fluids, 2020. **32**(12): p. 123317.
38. Quiñones, J.J., et al., *Prediction of respiratory droplets evolution for safer academic facilities*

planning amid COVID-19 and future pandemics: A numerical approach. Journal of Building Engineering, 2022. **54**: p. 104593.
39. Zaproudina, N., et al., *Reproducibility of infrared thermography measurements in healthy individuals.* Physiological measurement, 2008. **29**(4): p. 515.
40. Ai, Z., K. Hashimoto, and A.K. Melikov, *Airborne transmission between room occupants during short-term events: measurement and evaluation.* Indoor air, 2019. **29**(4): p. 563-576.
41. Li, X., et al. *Airborne transmission during short-term events: Direct route over indirect route*. in *Building Simulation*. 2022. Springer.
42. Nielsen, P.V. and C. Xu, *Multiple airflow patterns in human microenvironment and the influence on short-distance airborne cross-infection–A review.* Indoor and Built Environment, 2022. **31**(5): p. 1161-1175.
43. Villafruela, J., I. Olmedo, and J. San José, *Influence of human breathing modes on airborne cross infection risk.* Building and Environment, 2016. **106**: p. 340-351.
44. Xu, C., et al., *Human exhalation characterization with the aid of schlieren imaging technique.* Building and environment, 2017. **112**: p. 190-199.
45. Bolashikov, Z.D., M. Barova, and A.K. Melikov, *Wearable personal exhaust ventilation: Improved indoor air quality and reduced exposure to air exhaled from a sick doctor.* Science and Technology for the Built Environment, 2015. **21**(8): p. 1117-1125.
46. Yang, J., et al., *A time-based analysis of the personalized exhaust system for airborne infection control in healthcare settings.* Science and Technology for the Built Environment, 2015. **21**(2): p. 172-178.
47. Li, X., et al., *Airborne transmission of exhaled pollutants during short-term events: Quantitatively assessing inhalation monitor points.* Building and Environment, 2022. **223**: p. 109487.
48. Squires, K.D. and J.K. Eaton, *Preferential concentration of particles by turbulence.* Physics of Fluids A: Fluid Dynamics, 1991. **3**(5): p. 1169-1178.
49. Maxey, M.R., *The gravitational settling of aerosol particles in homogeneous turbulence and random flow fields.* Journal of fluid mechanics, 1987. **174**: p. 441-465.
50. Zemouri, C., et al., *Dental aerosols: microbial composition and spatial distribution.* Journal of Oral Microbiology, 2020. **12**(1): p. 1762040.
51. Ehtezazi, T., et al., *SARS-CoV-2: characterisation and mitigation of risks associated with aerosol generating procedures in dental practices.* British dental journal, 2021: p. 1-7.
52. Shahdad, S., et al., *Fallow time determination in dentistry using aerosol measurement in mechanically and non-mechanically ventilated environments.* British Dental Journal, 2021: p. 1-8.
53. Lahdentausta, L., et al., *Aerosol concentrations and size distributions during clinical dental procedures.* Heliyon, 2022. **8**(10): p. e11074.
54. Kuga, K., P. Wargocki, and K. Ito, *Breathing zone and exhaled air re-inhalation rate under transient conditions assessed with a computer-simulated person.* Indoor air, 2022. **32**(2): p. e13003.
55. To, K.K.-W., et al., *Consistent detection of 2019 novel coronavirus in saliva.* Clinical Infectious Diseases, 2020. **71**(15): p. 841-843.
56. Bennett, A., et al., *Microbial aerosols in general dental practice.* British dental journal, 2000. **189**(12): p. 664-667.

57. Dabiri, D., et al., *A multi-disciplinary review on the aerobiology of COVID-19 in dental settings.* Frontiers in dental medicine, 2021: p. 66.
58. Aydin, O., et al., *Performance of fabrics for home-made masks against the spread of COVID-19 through droplets: A quantitative mechanistic study.* Extreme Mechanics Letters, 2020. **40**: p. 100924.
59. Ge, Z.-y., et al., *Possible aerosol transmission of COVID-19 and special precautions in dentistry.* Journal of Zhejiang University-SCIENCE B, 2020. **21**(5): p. 361-368.
60. Ather, A., et al., *Coronavirus disease 19 (COVID-19): implications for clinical dental care.* Journal of endodontics, 2020. **46**(5): p. 584-595.
61. Bertolín, L.S., et al., *Optimal position of air purifiers in elevator cabins for the improvement of their ventilation effectiveness.* Journal of Building Engineering, 2023. **63**: p. 105466.
62. Rodríguez, M., et al., *Are the Portable Air Cleaners (PAC) really effective to terminate airborne SARS-CoV-2?* Science of The Total Environment, 2021. **785**: p. 147300.
63. Association, H.K.D. *UPDATES ON CLINIC MANAGEMENT FOR STAFF AND PATIENTS UNDER COVID-19*. 2022; Available from: https://hkda.org/download/pdf/2022/COVID19/UpdatesOnClinicManagementForStaffAndPatients_en.pdf.
64. Li, X., et al., *Design and analysis of an active daylight harvesting system for building.* Renewable Energy, 2019. **139**: p. 670-678.
65. Chaudhury, N.M.A., et al., *Changes in saliva rheological properties and mucin glycosylation in dry mouth.* Journal of dental research, 2015. **94**(12): p. 1660-1667.